ELSEVIER

Evaluation of zeolite A for the sorptive removal of Cs^+ and Sr^{2+} ions from aqueous solutions using batch and fixed bed column operations

A.M. El-Kamash *

Hot Laboratory Center, Atomic Energy Authority of Egypt, P.O. 13759, Inshas, Cairo, Egypt

Abstract

Zeolite A was chemically synthesized and evaluated, as inorganic ion exchange material, for the removal of cesium and strontium ions from aqueous solutions in both batch and fixed bed column operations. Batch experiments were carried out as a function of pH, initial ion concentration and temperature. Simple kinetic and thermodynamic models have been applied to the rate and isotherm sorption data and the relevant kinetic and thermodynamic parameters were determined from the graphical presentation of these models. Breakthrough data were determined in a fixed bed column at room temperature (298 K) under the effect of various process parameters like bed depth, flow rate and initial ion concentration. The results showed that the total metal ion uptake and the overall bed capacity decreased with increasing flow rate and increased with increasing initial ion concentrations and bed depth. The dynamics of the ion exchange process was modeled by bed depth service time (BDST) model. The sorption rate constants (K) were found to increase with increase in flow rate indicating that the overall system kinetics was dominated by external mass transfer in the initial part of the sorption process in the column.

1. Introduction

There are a number of liquid processes and waste streams at nuclear facilities that require treatment for process chemistry control reasons and/or the removal of radioactive contaminants. Cesium and strontium are the most abundant radionuclides in nuclear fission products that are routinely or accidentally released. They have relatively long half-life of about 30 years and are considered as hazardous elements for the environment. Different techniques such as chemical precipitation, ion exchange, and evaporation are used for the treatment of aqueous waste solutions containing these ions. Ion exchange technique has become one of the most commonly used treatment methods for such aqueous streams due to its simplicity, selectivity and efficiency. A wide range of materials having different chemical and physical properties, which can be naturally occurring or synthetic, is available for this technique. Inorganic ion exchange materials have emerged as an increasingly important replacement

or complement for conventional organic ion exchange resins, particularly in liquid radioactive waste treatment due to their radiation stability and greater selectivity for certain radiological important species, such as cesium and strontium. Several inorganic ion exchangers such as zeolites, sodium titanates, silicotitanates and hexacyanoferrates [1–24] are in use in nuclear sites for the treatment of nuclear wastes.

Ion exchange properties of zeolites have been received great attention, especially for application in radioactive liquid waste treatment [13–24]. The cationic radioisotopes, present in the liquid effluents of low and intermediate level liquid wastes, can be removed by the ion exchange with the Na^+ ions of the zeolites. These inorganic materials possess high exchange capacity, possible selectivity and specificity, good resistant to radiation, and have proven advantages with respect to immobilization and final disposal when compared with organic ion exchangers [25–32]. This study is an extension of our previous work [13], where synthetic zeolite A material was chemically prepared, completely characterized and preliminary tested as an inorganic ion exchange material for application in radioactive waste treatment. The present work deals with a series of experiments to assess the utility of this prepared material for the removal of Cs^+ and Sr^{2+}

* Tel.: +20 2 774 6063; fax: +20 2 462 0796.
  E-mail address: kamash20@yahoo.com.

ions from aqueous solutions under batch and continuous flow conditions in a fixed bed mode. The relevant data, with respect to kinetic and equilibrium of Cs^+-Na^+ and Sr^{2+}-Na^+ exchanges, have been obtained using simple kinetic and thermodynamic models. Breakthrough studies were also carried out to evaluate the effect of process parameters, such as inlet flow rate, adsorbent bed height and initial adsorbate concentration on the shape of breakthrough curves of the sorption of both ions onto prepared material. The dynamics of the sorption process was also modeled by bed depth service time (BDST) model.

2. Experimental

2.1. Chemicals and reagents

All the reagents used in this work were of AR grade chemicals and were used without further purification. Cesium and strontium were supplied as cesium chloride and strontium chloride, from Sigma–Aldrich Company. Stock solutions of the test reagents were prepared by dissolving CsCl and $SrCl_2 \cdot 6H_2O$ in distilled water.

2.2. Zeolite A preparation and characterization

The aluminosilicate framework of zeolite A was synthesized in its sodium form from mixture consisting of aqueous solutions of $NaAlO_2$, $Na_2O \cdot SiO_2$, and NaOH. The crystallinity and chemical composition of the prepared material were investigated using X-ray diffraction (XRD), X-ray fluorescence (XRF), and thermal analysis. Detailed descriptions of the preparation and characterization processes were presented in [13,14].

2.3. Batch sorption studies

Batch experiments were performed under kinetic and equilibrium conditions. To determine the pH range at which the maximum uptake of Cs^+ and/or Sr^{2+} ions would take place on zeolite A, a series of 50 mL test tubes each containing 10 mg of zeolite A was filled with 10 mL of a desired concentration (100 mg/L). The initial pH was adjusted to values ranging from 2.0 to 8.0 using dilute solution of hydrochloric acid or sodium hydroxide. The tubes were shacked for 3 h to attain equilibrium. Preliminary investigations showed that the sorption process of each studied ion was completed after 2 h. The suspension obtained was centrifuged to separate the solid from the liquid phase. The clear liquid phases obtained were diluted to an appropriate concentration range for the elemental analysis using Atomic Absorption Spectrophotometer (Buck scientific model VGP 210).

2.3.1. Kinetic experiments

Kinetic studies were performed at room temperature (298 K) using three different concentrations of 50, 100 and 150 mg/L for Cs^+ and/or Sr^{2+} ions. The experiments were also conducted at three different temperatures (298, 313 and 333 K) using an initial ion concentration of 100 mg/L. For these investigations,

100 mg of zeolite A was contacted with 100 mL solution containing known concentration of Cs^+ and/or Sr^{2+} ions and the solution in the beaker was kept stirred in a thermostat shaker adjusted at the desired temperature. A fixed volume (2 mL) of the aliquot was withdrawn as a function of time while the solution was being continuously stirred. Thus, the ratio of the volume of solution to the weight of zeolite A in the beaker does not change from the original ratio. The withdrawn solution was centrifuged to separate the zeolite A and a fixed volume (1 mL) of the clear solution was pipetted out for the determination of the amount of unsorbed metal ion still present in solution. The amount of ion sorbed at a time t, q_t (mg/g), was calculated using:

$$q_t = (C_0 - C_t)\frac{V}{m} \tag{1}$$

where C_0 and C_t are the initial and equilibrium concentrations (mg/L) of metal ion in solution, V the volume (L) and m is the weight (g) of the zeolite A.

2.3.2. Sorption equilibrium experiments

In the experiments of sorption isotherm measurements, 10 mL of the metal ion solution of varying concentrations (100–1000 mg/L) were agitated with 10 mg of zeolite A at different temperatures (298, 313, and 333 K) and at initial pH of 6.0. After the established contact time (3 h) was reached, aliquots of supernatants were withdrawn and the amount of the metal ion retained in the zeolite phase (mg/g) was estimated.

All batch experiments were carried out in duplicate and the mean values are presented.

2.4. Fixed bed sorption studies

Fixed bed sorption studies were conducted to evaluate the column performance for Cs^+ and Sr^{2+} ions removal on zeolite A. Experiments were conducted in a vertical down flow Perspex column of 1.0 cm inner diameter and 20.0 cm length packed with prepared zeolite A at optimum pH of 6.0. Influent feed flow rate was supplied and maintained throughout the experiment by the use of variable flow peristaltic pump. At the exit of the column, flow rate was also controlled so as to get steady state conditions in the column. Sampling of effluent was done at predetermined time intervals in order to investigate the breakthrough point. The effluent samples were filtered, diluted and analyzed for Cs^+ and Sr^{2+} concentrations. Effects of inlet feed flow rate (3.12 and 5.00 mL/min), zeolite A bed height (3.0, 4.5 and 6.0 cm) and initial Cs^+ and Sr^{2+} concentrations (50, 100 and 150 mg/L) was investigated on the performance of the breakthrough curves for the sorption of each studied ion.

3. Results and discussion

3.1. Effect of pH

The effect of pH on the sorption removal of Cs^+ and Sr^{2+} ions from aqueous chloride solutions using prepared zeolite A material was investigated over the pH range from 2.0 to 8.0. It
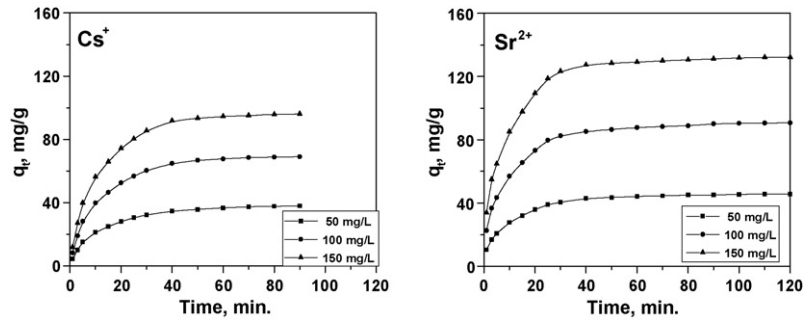
Fig. 1. Effect of initial ion concentration and contact time on the amount sorbed of Cs^+ and Sr^{2+} ions onto zeolite A.

was observed that each metal ion sorption process is dependent on the initial pH of the solution and the amount of metal ion sorbed increased with increase in the pH value. At lower values, the metal ion uptake was inhibited in this acidic medium and this can be attributed to the presence of H^+ ions competing with the Cs^+ and/or Sr^{2+} ions for the sorption sites. The uptake continuously increases with the increase in pH value and the highest uptake was observed at pH range from 6.0 to 8.0. It is also known that mineral acids affect the structure of zeolites. In the zeolite framework, the Si–O–Al is weaker than Si–O–Si and can easily be attached by H^+ ions affecting the zeolite structure. This defect is more so in the case of zeolites with low Si/Al ratios such as zeolite A and X types [33]. The extent of the damage to their structure depends on the pH of the acids. The structure of zeolites, particularly with low Si/Al ratios, may collapse in the presence of acids with pH lower than 5.0, but the severity would be more below pH value of 3.0. In fact, pH less than 5.0 is not recommended for zeolites [34]. So, all future sorption experiments in this work were carried out at initial pH value of 6.0.

3.2. Kinetic sorption studies

Preliminary investigations on the sorption rate of the studied ions by zeolite A indicated that the process is quite rapid and typically 80–90% sorption of the equilibrium value for each ion occurred within 30 min. The initial rapid sorption subsequently gives way to a slow approach to equilibrium, and equilibrium is reached in about 90–120 min.

3.2.1. Effect of initial concentration and contact time

The effect of the initial ion concentration was performed at initial concentrations of 50, 100 and 150 mg/L at 298 K for the sorption of Cs^+ and Sr^{2+} ions onto zeolite A and the results were shown in Fig. 1. It is clear that the sorption amount of both ions increases with increasing the initial ion concentration, and the amount of Sr^{2+} ions sorbed is grater than that of Cs^+ ions. Also, the amount of each metal ion sorbed sharply increases with time in the initial stage (0–40 min range), and then gradually increases to reach an equilibrium value in approximately 90–120 min. A further increase in contact time had a negligible effect on the amount of ion sorption. The equilibrium time was found to be independent of the initial concentration. According to these results, the agitation time was fixed at 3 h for the rest of the batch experiments to make sure that the equilibrium was reached. The increase in the uptake capacity of the zeolite material with increasing initial ion concentration may be due to higher probability of collision between each investigated ion and the zeolite particles. The variation in the extent of sorption may also be due to the fact that initially all sites on the surface of zeolite A were vacant and the metal ion concentration gradient was relatively high. Consequently, the extent of each ion uptake decreases significantly with the increase of contact time, depending on the decrease in the number of vacant sites on the surface of zeolite material.

3.2.2. Sorption kinetic modeling

Fig. 2 shows the variation of the amounts of Cs^+ and Sr^{2+} ions sorbed at different time intervals, for the fixed initial ion con-
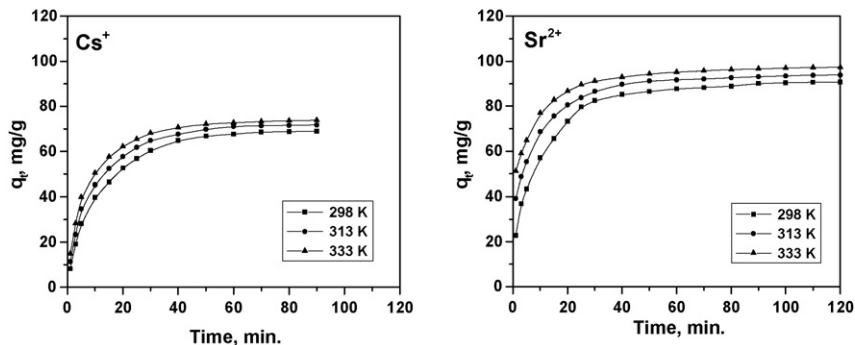

Fig. 2. Effect of contact time on the amount sorbed of Cs^+ and Sr^{2+} ions sorbed onto zeolite A at different temperatures.
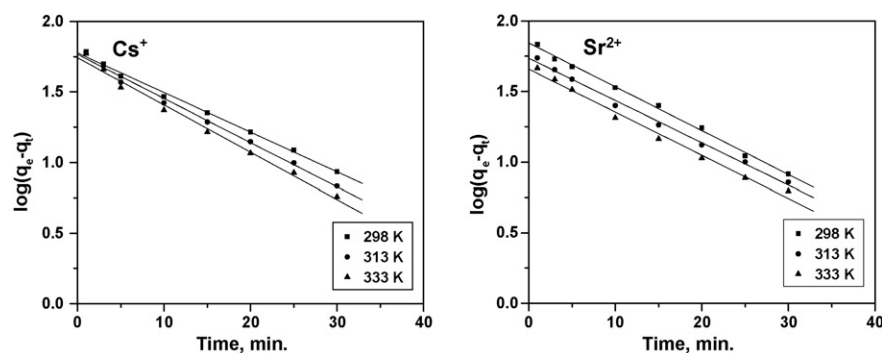
Fig. 3. Pseudo first-order kinetic plots for the sorption of Cs$^+$ and Sr^{2+} ions sorbed onto zeolite A at different temperatures.

centration of 100 mg/L and at different sorption temperatures of 298, 313 and 333 K. The data showed that the amount of the sorbed Cs$^+$ and Sr^{2+} ions increases with the increase in temperature indicating an endothermic nature of the sorption processes, while the time required reaching equilibrium remained practically unaffected. Also, the amount recovery of each ion from the solution increases with time, and attained equilibrium within 90–120 min.

It is well recognized that the characteristic of the sorbent surface is a critical factor that affect the sorption rate parameters and that diffusion resistance plays an important role in the overall transport of the ions. To describe the changes in the sorption of metal ions with time, three simple kinetic models were tested. The rate constant of each metal ion removal from the solution by zeolite A was determined using pseudo first-order and pseudo second-order rate models. The Lagergren pseudo first-order expression is written as [35].

$$\log(q_e - q_t) = \log q_e - \frac{k_1}{2.303}t \tag{2}$$

where q_e and q_t (mg/g) are the amount of metal ion sorbed onto zeolite A at equilibrium and at time t, respectively and k_1 is the pseudo first order rate constant (min^{-1}).

The slopes and intercept of the plots of $\log(q_e - q_t)$ versus t, as shown in Fig. 3, were used to determine the first order rate constant (k_1) and the theoretical equilibrium sorption capacities (q_e), respectively. The calculated values of k_1 and q_e with the values of the linear correlation coefficients (R^2) of each plot are presented in Table 1. Straight lines obtained from the pseudo first-order kinetic plots suggest the applicability of the pseudo first-order

kinetic model to fit the experimental data over the initial stage of the sorption process (20–30 min). But it is also required that theoretically calculated equilibrium sorption capacities, q_e, should be in accordance with the experimental sorption capacity values. As can be seen from Table 1, although the linear correlation coefficients of the plots are so good, the q_e (calculated) values are not in agreement with q_e (experimental) for all studied sorption processes. So, it could suggest that the sorption of both metal ions onto zeolite A is not a first-order reaction.

The pseudo second-order rate model is expressed as [36,37]:

$$\frac{t}{q_t} = \frac{1}{k_2 q_e^2} + \frac{1}{q_e}t \tag{3}$$

where k_2 is the rate constant of pseudo second-order equation (g/mg min).

The kinetic plots of t/q_t versus t for both Cs$^+$ and Sr^{2+} ions sorption at different temperatures are presented in Fig. 4. The relation is linear, and the correlation coefficient (R^2), suggests a strong correlation between the parameters and also explains that the sorption process of each ion follows pseudo second-order kinetics. The product $k_2 q_e^2$ is the initial sorption rate represented as $h = k_2 q_e^2$. From Table 1, it can be shown that the values of the initial sorption rate (h) and rate constant (k_2) were increased with the increase in temperature. The correlation coefficient R^2 has an extremely high value (>0.99), and its calculated equilibrium sorption capacity (q_e) is consistent with the experimental data. These results explain that the pseudo second-order sorption mechanism is predominant and that the overall rate constant of each sorption process appears to be controlled by the chemical sorption process [37].

Table 1
The calculated parameters of the pseudo first-order and pseudo second-order kinetic models for Cs$^+$ and Sr^{2+} ions sorbed onto zeolite A at different sorption temperatures

| Metal ion	Temperature (K)	First-order kinetic parameters			Second-order kinetic parameters				$q_{e, exp.}$ (mg/g)
		k_1 (min^{-1})	$q_{e, calc.}$ (mg/g)	R^2	k_2 (g/mg min)	$q_{e, calc.}$ (mg/g)	h (mg/g min)	R^2	
Cs$^+$	298	0.0647	55.20	0.997	0.0015	76.69	8.88	0.999	69.00
	313	0.0721	58.30	0.996	0.0020	77.70	12.05	0.999	71.70
	333	0.0771	59.80	0.995	0.0026	78.25	15.99	0.999	73.80
Sr^{2+}	298	0.0716	69.78	0.998	0.0020	94.97	18.30	0.999	90.70
	313	0.0691	54.33	0.997	0.0031	96.52	29.08	0.999	93.80
	333	0.0704	45.54	0.990	0.0041	99.20	40.16	0.999	97.30
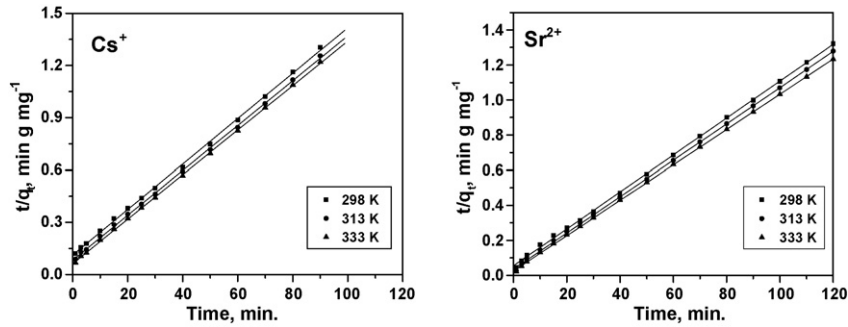
Fig. 4. Pseudo second-order kinetic plots for the sorption of Cs^+ and Sr^{2+} ions sorbed onto zeolite A at different temperatures.
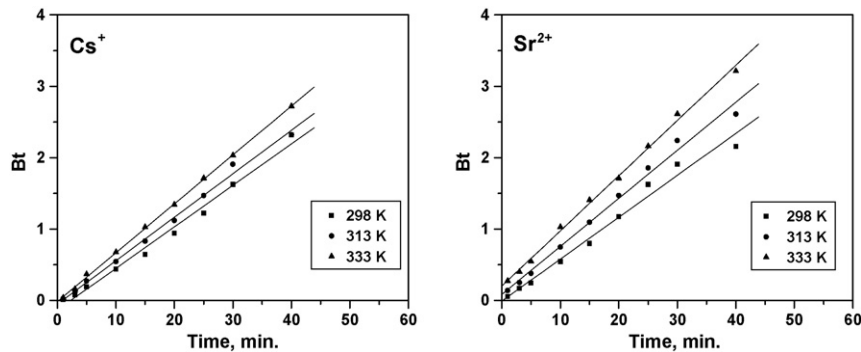

Fig. 5. Plot of Bt vs. time for the sorption of Cs^+ and Sr^{2+} ions sorbed onto zeolite A at different temperatures.

In order to identify the step governing the overall removal rate of the sorption process, the model given by Boyd et al. [38,39] was applied. In this model, various parameters were calculated using the following expressions:

$$F(t) = 1 - \frac{6}{\pi^2} \sum_{n=1}^{\infty} \frac{1}{n^2} \exp\left(-\frac{D_i \pi^2 t n^2}{r_0^2}\right) \tag{4}$$

$$F(t) = 1 - \frac{6}{\pi^2} \sum_{n=1}^{\infty} \frac{1}{n^2} \exp(-n^2 Bt) \tag{5}$$

$$B = \frac{\pi^2 D_i}{r_0^2} \tag{6}$$

where F is the fractional attainment of equilibrium at time t ($F = q_t/q_e$), B the time constant, D_i the effective diffusion coefficient of metal ion, r_0 the radius of the zeolite particle (0.25 mm), and n is integers 1, 2, 3, ...

The Bt values in Eq. (5) for values of F were obtained from Reichenberg's table [40]. The linearity test of Bt versus time plots is employed to distinguish between film and particle dif-fusion controlling sorption process. If the plot is a straight line passing through the origin, then the sorption rate is governed by particle diffusion mechanism otherwise it is governed by film diffusion. Fig. 5 depicts the Bt versus time plots for Cs^+ and Sr^{2+} ions at different temperatures. The plots are linear and pass through the origin for both ions, indicating that the sorption process to be particle diffusion at all studied temperatures. The values of D_i calculated at different temperatures for Cs^+ and Sr^{2+} ions are presented in Table 2. The magnitude of the diffusion coefficient is dependent upon the nature of the sorption process. For physical adsorption, the value of the effective diffusion coefficient ranges from 10^{-6} to 10^{-9} m²/s and for chemisorption, the value ranges from 10^{-9} to 10^{-17} m²/s [41]. The difference in the values is due to the fact that in physical adsorption the molecules are weakly bound and therefore there is ease of migration, whereas for chemisorption the molecules are strongly bound and mostly localized. Therefore, from this research, the most likely nature of sorption is chemisorption since the values of D_i were in the order 10^{-12} m²/s for both ions.

On the other hand, plotting of $\ln D_i$ versus $1/T$ gave a straight line (figure not shown) proves the validation of the linear form

Table 2
Diffusion coefficient and thermodynamic parameters for the sorption of Cs^+ and Sr^{2+} onto zeolite A

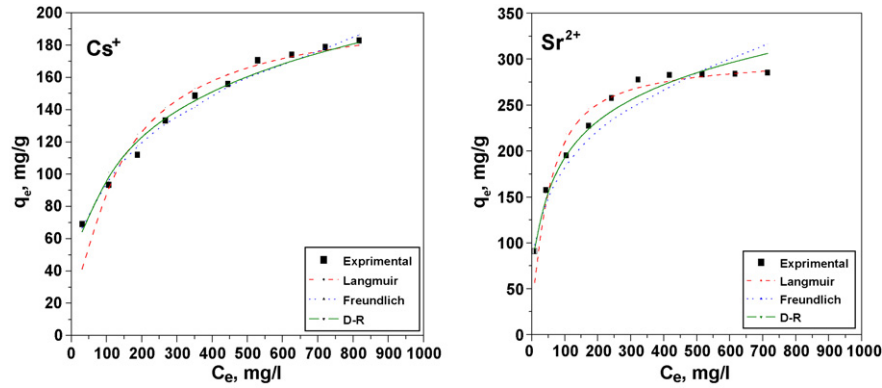| Metal ion	$D_i \times 10^{12}$ (m²/s)			R^2			$D_0 \times 10^8$ (m²/s)	E_a (kJ/mol)	R^2	ΔS^* (J/mol K)
	298 K	313 K	333 K	298 K	313 K	333 K				
Cs^+	6.45	7.21	9.44	0.994	0.997	0.999	2.44	9.06	0.982	−81.58
Sr^{2+}	6.50	8.13	11.29	0.991	0.995	0.998	12.50	13.05	0.991	−67.99

Fig. 6. Sorption isotherm of Cs+ and Sr2+ions sorbed onto zeolite A at 298 K. The solid and dashed lines represent the fitting data by Freundlich, Langmuir, and D–R isotherm models.

of Arrhenius equation:

$$\ln D_i = \ln D_0 - \left(\frac{E_a}{RT}\right) \tag{7}$$

where D_0 is a pre-exponential constant analogous to Arrhenius frequency factor.

The activation energies for both ions, E_a, were calculated from the slope of the straight lines and the obtained values were presented in Table 2. Values of $E_a < 42.0$ kJ/mol generally indicate diffusion-control processes and higher values represent chemical reaction processes [42]. Such a low value of the activation energy for the sorption of each metal ion indicates a chemical sorption process consisting of weak interaction between sorbent (zeolite A) and sorbate (Cs+ and/or Sr2+) and illustrate that each sorption process has a low potential energy.

The Arrhenius equation would be also used to calculate D_0 which in turn is used for the calculation of activation entropy, ΔS^*, of the sorption process using:

$$D_0 = 2.72 \left(\frac{kTd^2}{h}\right) \exp^{\Delta S^*/R} \tag{8}$$

where k is the Boltzmann constant, h the Planks constant, d the average distance between two successive positions, R the gas constant and T is the absolute temperature. Assuming that the value of d is equal to 5×10^{-8} cm [14], the values of ΔS^* for both the ions were calculated and presented in Table 2. The value of entropy of activation (ΔS^*) is an indication of whether or not

the reaction is an associative or dissociative mechanism. ΔS^* values > -10 J/mol K generally imply a dissociative mechanism [42]. However, the high negative values of ΔS^* obtained in this study, suggested that both Cs+ and Sr2+ ions sorption onto zeolite A is an associative mechanism and normally reflect that no significant change occurs in the internal structure of the zeolite matrix during the sorption of ions.

3.3. Sorption isotherms

Sorption equilibrium is usually described by an isotherm equation whose parameters express the surface properties and affinity of the sorbent, at a fixed temperature and pH. An adsorption isotherm describes the relationship between the amount of adsorbate on the adsorbent and the concentration of dissolved adsorbate in the liquid at equilibrium [43]. In this concern, the sorption isotherms for the removal of Cs+ and Sr2+ ions from aqueous chloride solutions onto synthetic zeolite A at three different temperatures were determined. Fig. 6 shows, as a representative, the experimental and fitted isotherm data by Langmuir, Freundlich, and Dubinin–Radushkviech (D–R) isotherm models at 298 K. The isotherms are regular, positive, and concave to the concentration axis for both ions. The initial rapid sorption gives way to a slow approach to equilibrium at higher ion concentrations.

Several common sorption isotherm models including Langmuir, Freundlich, and Dubinin–Radushkviech (D–R) isotherm models were considered to fit the obtained isotherm data.
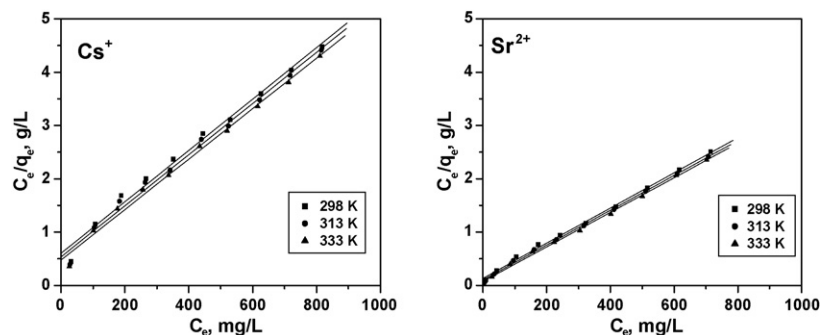

Fig. 7. Langmuir isotherm plots for the sorption of Cs+ and Sr2+ions sorbed onto zeolite A at different temperatures.

Table 3
Langmuir and Freundlich isotherm parameters for the sorption of Cs^+ and Sr^{2+} onto zeolite A

Metal ion	Temperature (K)	Langmuir model parameters				Freundlich model parameters		
		Q^o (mg/g)	$b \times 10^3$ (L/mg)	R^2	R_L	n	K_f (mg/g)	R^2
	298	207.47	8.00	0.995	0.111	3.15	22.43	0.994
Cs^+	313	208.77	8.96	0.995	0.100	3.29	25.02	0.991
	333	211.41	9.93	0.996	0.091	3.38	27.29	0.991
	298	303.00	24.75	0.999	0.040	3.73	54.61	0.982
Sr^{2+}	313	305.81	31.88	0.999	0.031	4.12	65.85	0.982
	333	308.64	43.28	0.999	0.022	4.81	83.46	0.987

3.3.1. Langmuir isotherm model

Langmuir sorption isotherm models the monolayer coverage of the sorption surfaces and assumes that sorption occurs on a structurally homogeneous adsorbent and all the sorption sites are energetically identical. The linearized form of the Langmuir equation is given by:

$$\frac{C_e}{q_e} = \frac{1}{Q^o b} + \frac{1}{Q^o} C_e \qquad (9)$$

where q_e is the amount of metal ion sorbed per unit weight of zeolite A (mg/g), C_e the equilibrium concentration of the metal ion in the equilibrium solution (mg/L), Q^o the monolayer adsorption capacity (mg/g) and b is the constant related to the free energy of adsorption ($b \propto e^{-\Delta G/RT}$).

The graphic presentations of (C_e/q_e) versus C_e give straight lines for both Cs^+ and Sr^{2+} ions sorbed onto zeolite A, as presented in Fig. 7, confirming that this expression is indeed a reasonable representation of chemisorption isotherm. The numerical value of constants Q^o and b evaluated form the slope and intercept of each plot are given in Table 3. The value of saturation capacity Q^o corresponds to the monolayer coverage and defines the total capacity of the adsorbent for a specific metal ion. As it can be seen from Table 3, the monolayer sorption capacity (Q^o) values of zeolite A towards Sr^{2+} ions are relatively higher than that of Cs^+ ions. The Langmuir constants Q^o and b for the sorption of both ions increased with temperature showing that the sorption capacity and intensity of sorption are enhanced at higher temperatures. This increase in sorption capacity with temperature suggested that the active surface available for sorption has increased with temperature.

One of the essential characteristics of the Langmuir model could be expressed by dimensionless constant called equilibrium parameters R_L [44]

$$R_L = \frac{1}{1 + bC_0} \qquad (10)$$

where C_0 is the highest initial metal ion concentration (mg/L). The value of R_L indicates the type of isotherm to be irreversible ($R_L = 0$), favorable ($0 < R_L < 1$), linear ($R_L = 1$), or unfavorable ($R_L > 1$). All the R_L values (Table 3) were found to be less than 1 and greater than 0 indicating the favorable sorption isotherms of both metal ions.

3.3.2. Freundlich isotherm model

Freundlich equation is derived to model the multilayer sorption and for the sorption on heterogeneous surfaces. The logarithmic form of Freundlich equation may be written as:

$$\log q_e = \log K_f + \frac{1}{n} \log C_e \qquad (11)$$

where K_f is constant indicative of the relative sorption capacity of zeolite A (mg/g) and $1/n$ is the constant indicative of the intensity of the sorption process. The pictorial illustration of $\log q_e$ versus $\log C_e$ is shown in Fig. 8, which suggests that the sorption of Cs^+ and Sr^{2+} ions obeys Freundlich isotherm over the entire range of sorption concentration studied. The numerical values of the constants $1/n$ and K_f are computed from the slope and the intercepts, by means of a linear least square fitting method, and also given in Table 3. It can be seen from these data that the Freundlich intensity constant (n) are greater than unity for both studied ions. This has physicochemical significance with reference to the qualita-
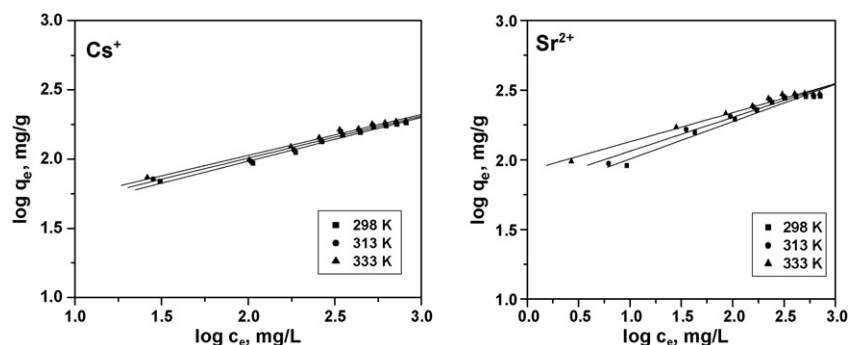

Fig. 8. Freundlich isotherm plots for the sorption of Cs^+ and Sr^{2+} ions sorbed onto zeolite A at different temperatures.
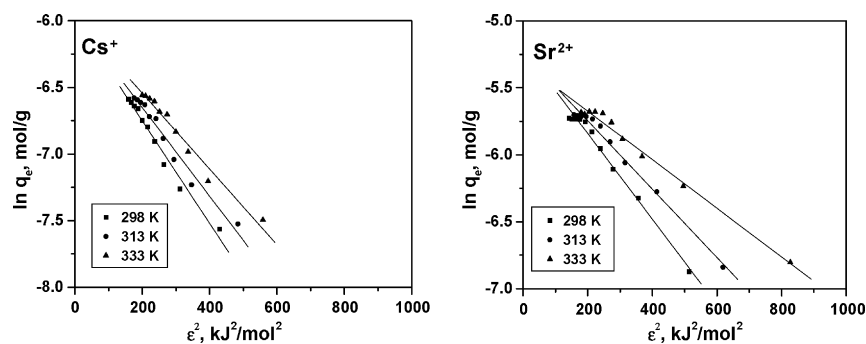
Fig. 9. D–R isotherm plots for the sorption of Cs$^+$ and Sr^{2+}ions sorbed onto zeolite A at different temperatures.

tive characteristics of the isotherms, as well as to the interactions between metal ions species and zeolite A. In our case, $n > 1$ for both ion species, the zeolite A shows an increase tendency for sorption with increasing solid phase concentration. This should be attributed to the fact that with progressive surface coverage of adsorbent, the attractive forces between the metal ion species such as van der Waals forces, increases more rapidly than the repulsive forces, exemplified by short-range electronic or long-range Coulombic dipole repulsion, and consequently, the metal ions manifest a stronger tendency to bind to the zeolite A site [13,45].

3.3.3. Dubinin–Radushkviech isotherm (D–R isotherm)

In order to study the nature of the sorption processes, the D–R isotherm was also verified in the form [43]:

$$\ln q_e = \ln q_m - \beta \varepsilon^2 \tag{12}$$

where q_m is the maximum amount of ion that can be sorbed onto unit weight zeolite A, i.e. sorption capacity (mmol/g), β the constant related to the sorption energy (mol^2/kJ^2); and ε is the Polanyi potential $= RT \ln(1 + 1/C_e)$, where R is the gas constant (kJ/mol K), and T is the absolute temperature (K).

The mean free energy of sorption is the free energy change when one mole of ion is transferred to the surface of zeolite A from infinity in the solution, and it is calculated from:

$$E = (-2\beta)^{-1/2} \tag{13}$$

The magnitude of E can be related to the reaction mechanism. If E is in the range of 8–16 kJ/mol, sorption is governed by ion exchange [38]. In the case of $E < 8.0$ kJ/mol, physical forces may affect the sorption mechanism.

The D–R plots of $\ln q_e$ versus ε^2 for the sorption of both ions at different temperatures are given in Fig. 9. These linear plots indicate that the D–R isotherm expression is followed for

each metal ion. Linear regression analysis using paired of $\ln q_e$ and ε^2 resulted in the derivation of q_m, β, E and the correlation factor (R^2). The correlation factor is a statistical measure of how well the data points fit the regression line. These D–R parameters are presented in Table 4. The values of the mean free energy, E, of sorption is in all cases in the range of 8–16 kJ/mol, which are within the energy ranges of ion exchange reaction [38]. The maximum sorption capacities (q_m) are in that ranges of 2.51–2.54 and 4.90–5.51 mmol/g for Cs$^+$ and Sr^{+2} ions, respectively. These values are considerably less than the theoretical exchange capacity (CEC) calculated from the chemical formula of zeolite A (5.45 meq/g). This could be due to the size window of the zeolite A and to the radius of Cs$^+$ and/or Sr^{2+} ions, which make difficult the ion exchange and therefore the values determined experimentally were lower [13].

3.3.4. Effect of temperature

In order to gain insight into the thermodynamic nature of the sorption process, several thermodynamic parameters for the present systems were calculated. The Gibbs free energy change, ΔG°, is the fundamental criterion of spontaneity. Reactions occur spontaneously at a given temperature if ΔG° is a negative quantity. The free energy of the sorption reaction is given by the following equation:

$$\Delta G^\circ = -RT \ln K_c \tag{14}$$

where K_c is the sorption equilibrium constant, R the gas constant and T is the absolute temperature (K).

The values of the thermodynamic equilibrium constant (K_c) at different studied temperatures were determined from the product of the Langmuir equation parameters Q° and b [46]. The variation of K_c with temperature, as summarized in Table 5, showed that K_c values increase with increase in sorption temperature, thus implying a strengthening of adsorbate–adsorbent interac-

Table 4
D–R isotherm parameters of Cs$^+$ and Sr^{2+}ions sorbed zeolite A

Temperature (K)	β (mol^2/kJ^2)		q_m (mmol/g)		R^2		E (kJ/mol)	
	Cs$^+$	Sr^{2+}	Cs$^+$	Sr^{2+}	Cs$^+$	Sr^{2+}	Cs$^+$	Sr^{2+}
298	−0.00385	−0.00321	2.515	4.900	0.989	0.985	11.40	12.50
313	−0.00333	−0.00255	2.526	5.320	0.986	0.991	12.25	13.86
333	−0.00284	−0.00211	2.543	5.510	0.987	0.986	13.27	15.43

Table 5
Values of the thermodynamic parameters for the sorption of Cs^+ and Sr^{2+} ions onto zeolite A

Temperature (K)	K_C		ΔG° (kJ/mol)		ΔH° (kJ/mol)		ΔS° (J/mol K)	
	Cs^+	Sr^{2+}	Cs^+	Sr^{2+}	Cs^+	Sr^{2+}	Cs^+	Sr^{2+}
298	1.66	7.50	−1.256	−4.992	5.57	13.72	22.91	62.70
313	1.87	9.75	−1.629	−5.926				
333	2.10	13.36	−2.054	−7.177				

tions at higher temperature. Also, the obtained negative values of ΔG° confirm the feasibility of the process and the spontaneous nature of the sorption processes with preference towards Sr^{2+} than Cs^+ ions. Other thermal parameters such as enthalpy change (ΔH°), and entropy change (ΔS°) were calculated using the relationships:

$$\ln K_c = \frac{\Delta S^\circ}{R} - \frac{\Delta H^\circ}{RT} \tag{15}$$

The values of enthalpy change (ΔH°) and entropy change (ΔS°) calculated from the slope and intercept of the plot of $\ln K_c$ versus $1/T$ (figure not shown) are also given in Table 5. The change in ΔH° for both ions was found to be positive confirming the endothermic nature of the sorption processes. ΔS° values were found to be positive due to the exchange of the metal ions with more mobile ions present on zeolite A, which would cause increase in the entropy during the sorption process.

3.4. Column studies

Batch experimental data are often difficult to apply directly to the fixed bed sorption column because isotherms are unable to give accurate data for scale up since a flow in the column is not at equilibrium. Fixed bed column sorption experiments were carried out to study the sorption dynamics. The fixed bed column operation allows more efficient utilization of the sorptive capacity than the batch process. The shape of the breakthrough curve and the time for the breakthrough appearance are the predominant factors for determining the operation and the dynamic response of the sorption column. The general position of the breakthrough curve along the volume/time axis depends on the capacity of the column with respect to bed height, the feed concentration and flow rate [47–52].

The effects of process variables on the zeolite A column performance were studied; these include bed depth, flow rate and initial Cs^+ and/or Sr^{2+} concentrations. The two different flow rates were 3.12 and 5.00 mL/min. The studied bed depths were 3.0, 4.5, and 6.0 cm and the initial ion concentrations are 50, 100 and 150 mg/L. In this concern, the loading behavior of Cs^+ and Sr^{2+} ions sorbed onto zeolite A from aqueous chloride solutions in a fixed bed are shown by breakthrough curves that are expressed in terms of normalized concentration defined as the ratio of effluent ion concentration to its inlet concentration (C_t/C_0) as a function of effluent volume for a given bed height. The total sorbed ion quantity (q_{tot}, mg) in the column, for a given feed concentration (C_0, mg/L) and flow rate (Q, mL/min), can be found by calculating the area under the breakthrough curve obtained by integrating the sorbed ion concentration (C_{ads}, mg/L) versus time plot (Eq. (16)).

$$q_{tot} = \frac{Q}{1000} \int_0^{tot} C_{ads}\, dt = \frac{Q}{1000} \int_0^{tot} (C_0 - C_t)\, dt \tag{16}$$

The total amount of ion fed to the column (X, mg) is calculated from the following equation:

$$X = \frac{C_0 V_{eff}}{1000} \tag{17}$$

The total percent removal of the ion by the column, i.e. the column performance by zeolite A can be calculated from the following equation:

$$\text{total ion removal } (\%) = \frac{q_{tot}}{X} \times 100 \tag{18}$$

3.4.1. Effect of bed depth

The breakthrough curves obtained for Cs^+ and Sr^{2+} ions sorption onto zeolite A at different bed depths (3.0, 4.5, and 6.0 cm) for a constant linear flow rate of 3.12 mL/min and at 100 mg/L
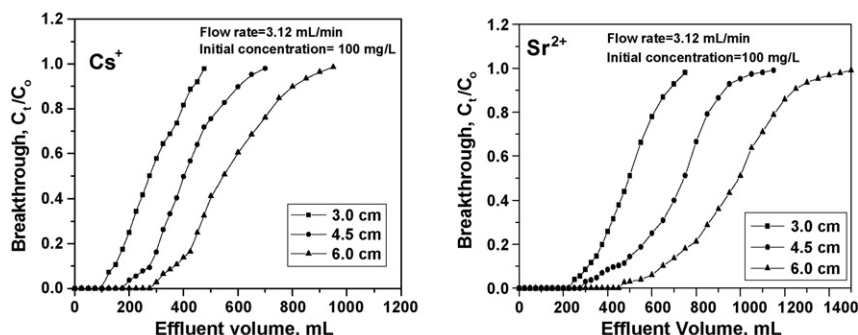

Fig. 10. Breakthrough curves for Cs^+ and Sr^{2+} ions sorbed onto zeolite A at different bed depth and at 3.12 mL/min flow rate.

Table 6
Fixed bed data of Cs$^+$ and Sr^{2+} ions sorbed onto zeolite A at different process parameters

Metal ion	C_o (mg/L)	Q (mL/min)	Z (cm)	X (mg)	q_{tot} (mg)	Column performance (%)	Bed capacity (mg/g)
	50.0	3.12	3.0	40.0	27.8	69.4	27.8
			3.0	50.0	32.5	65.0	32.5
		3.12	4.5	70.0	50.0	71.4	33.3
			6.0	95.0	75.0	78.9	37.5
Cs$^+$	100.0		3.0	45.0	25.0	55.5	25.0
		5.00	4.5	65.0	41.5	63.8	27.6
			6.0	90.0	63.0	70.0	31.5
	150.0	3.12	3.0	60.0	33.8	65.3	33.8
	50.0	3.12	3.0	60.0	44.5	74.1	44.5
			3.0	75.0	52.5	70.0	52.5
		3.12	4.5	115.0	87.5	76.0	58.3
			6.0	140.0	121.0	86.4	60.5
Sr^{2+}	100.0		3.0	60.0	40.0	66.7	40.0
		5.00	4.5	90.0	64.0	71.0	42.6
			6.0	120.0	94.8	79.0	47.4
	150.0	3.12	3.0	83.0	53.5	64.5	53.5

Table 7
BDST model parameters of Cs$^+$ and Sr^{2+} ions sorbed onto zeolite A at different bed deaths and flow rates

Metal ion	Q (mL/min)	Z (cm)	Time to 10% breakthrough (min)	N_0 (mg/mL)	N_0 (mg/g)	$K \times 10^4$ (L/mg min)	Z_0 (cm)
		3.0	48				
	3.12	4.5	88	9.53	13.42	9.69	0.94
		6.0	120				
Cs$^+$		3.0	20				
	5.00	4.5	45	8.92	12.56	9.09	1.61
		6.0	65				
		3.0	100				
	3.12	4.5	144	14.29	20.13	19.41	0.31
		6.0	208				
Sr^{2+}		3.0	55				
	5.00	4.5	80	13.79	19.43	17.62	0.58
		6.0	120				

initial Cs$^+$ and Sr^{2+} concentrations are shown in Fig. 10. The results indicate that the volume of breakthrough varies with bed depth. The bed capacity and the percent removal (column performance) of both Cs$^+$ and Sr^{2+} ions increased with increasing bed height (Table 6), as more binding sites were available for sorption. The increase in the ion sorption with bed depth was due to the increase in the sorbent doses in larger beds, which provided greater sorption sites for Cs$^+$ and Sr^{2+} ions. The breakthrough time also increased with bed depth,

suggesting that it is the determining parameter of the process (Table 7).

3.4.2. Effect of flow rate

The effect of flow rate on Cs$^+$ and Sr^{2+} ions sorption by zeolite A was investigated by varying the flow rate from 3.12 to 5.00 mL/min and keeping the initial Cs$^+$ and/or Sr^{2+} concentration (100 mg/L) for the same previous studied bed depths. The plots of the breakthrough curves of Cs$^+$ and Sr^{2+} ions at vari-
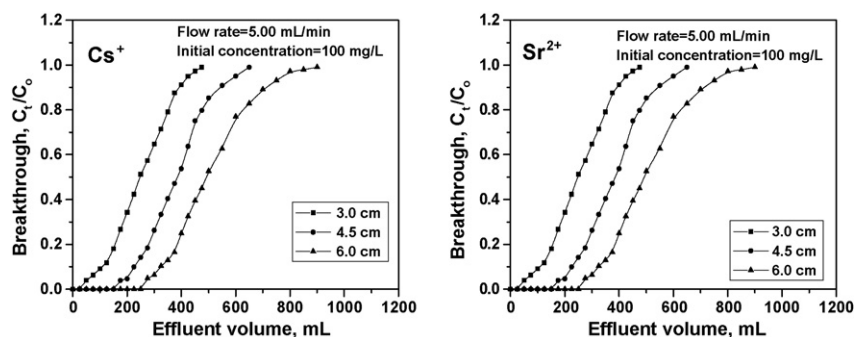

Fig. 11. Breakthrough curves for Cs$^+$ and Sr^{2+} ions sorbed onto zeolite A at different bed depth and at 5.00 mL/min flow rate.
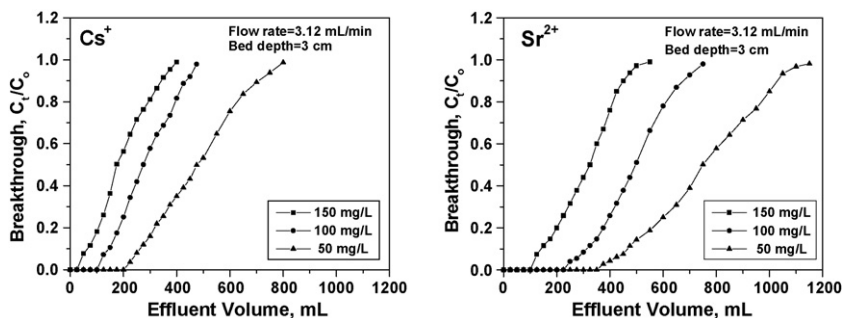
Fig. 12. Breakthrough curves for Cs$^+$ and Sr^{2+} ions sorbed onto zeolite A at different initial ion concentrations.

ous flow rates are shown in Figs. 10 and 11. The total sorbed ion quantities, treated volume at breakthrough, breakthrough times and metal ion removal percents with respect to each flow rate were evaluated from the sorption data and are presented in Tables 6 and 7. As is evident from these results, an increase in the flow rate reduces the volume treated efficiently until breakthrough and thereby decreases the service time of the bed. This is due to the decrease in the residence time of the Cs$^+$ and Sr^{2+} ions within the bed at higher flow rates. Much sharper breakthrough curves for Cs$^+$ and Sr^{2+} ions sorption onto zeolite A were obtained at higher flow rates. The breakthrough time and the amount of total Cs$^+$ and Sr^{2+} sorbed also decreased with increasing flow rate. This is certainly because of the reduced contact time causing a weak distribution of the liquid inside the column, which leads to a lower diffusivity of the solute among the particles of the zeolite A [49].

3.4.3. Effect of initial ion concentration

The sorption performance of zeolite A column was investigated at different initial Cs$^+$ and Sr^{2+} concentrations. The effect of varying the initial Cs$^+$ and/or Sr^{2+} concentrations from 50 to 150 mg/L at a flow rate of 3.12 mL/min and bed depth of 3.0 cm are illustrated in Fig. 12. The total sorbed Cs$^+$ and Sr^{2+} quantities, treated volume at breakthrough, breakthrough times and removal percents with respect to the initial Cs$^+$ and/or Sr^{2+} concentration were evaluated from the sorption data and are also presented in Tables 6 and 7. As is evident from these tables, with the rise in the initial Cs$^+$ and/or Sr^{2+} concentration, the volume of solution treated before breakthrough reduces considerably. This is due to the fact that a high metal ion concentration easily saturates the column bed, thereby decreasing the breakthrough time. The main driving force for the sorption process is the concentration difference between the metal ion in the solution and in the sorbent. This may explain the reason why higher sorbed Cs$^+$ and Sr^{2+} quantities were obtained at higher metal ion feed concentrations [50].

3.4.4. Modeling of breakthrough curves

The most important criterion in the design of fixed bed sorption systems is the prediction of fixed bed column breakthrough or the shape of the sorption wave front, which determines the operation life span of the bed. The dynamics of the sorption process was studied using bed depth service time (BDST) method based on a model proposed by Bohart and Adams [51]. This model assumes that the sorption rate is proportional to both the residual capacity of the sorbent and the concentration of the sorbate species. The Adams–Bohart model is used only for the description of the initial part of the breakthrough curve, i.e. up to the breakpoint or 10–50% of the saturation points [52].

According to Bohart–Adams model, the relationship between t and Z is described as in the following equation [47–52].

$$t = \frac{N_0 Z}{C_0 U_0} - \frac{1}{KC_0} \ln\left(\frac{C_0}{C_t} - 1\right) \qquad (19)$$

where C_t is the effluent concentration of metal ion (mg/L), C_0 the initial ion concentration (mg/L), t the breakthrough service time, N_0 the volumetric adsorption capacity (mg/L), Z the bed depth of the column (cm), U_0 the linear flow velocity of feed to bed (cm/min) and K is the sorption rate constant (L/mg min).

The equation of a straight line on BDST curve is expressed as in the form of:

$$t = mZ + b \qquad (20)$$

where m is the slope, and b is the ordinate intercept represented by:

$$m = \frac{N_0}{C_0 U_0}, \quad \text{and} \quad b = -\frac{1}{KC_0} \ln\left(\frac{C_0}{C_t} - 1\right) \qquad (21)$$

The critical bed depth (Z_0) is obtained for $t = 0$ and for a fixed outlet concentration $C_t = C_b$, where C_b is the breakthrough concentration defined as a limit concentration or a fixed percent of initial concentration:

$$Z_0 = \frac{U_0}{KN_0} \ln\left(\frac{C_0}{C_b} - 1\right) \qquad (22)$$

The critical bed depth (Z_0) represents the theoretical depth of sorbent, necessary to prevent the sorbate concentration to exceed the limit concentration C_b.

The BDST sorption model was applied to the present experimental data to study the breakthrough behavior of Cs$^+$ and Sr^{2+} onto zeolite A and to estimate the characteristic parameters, K and N_0 from the model. Applying Eq. (19) to the experimental data at different bed depths and flow rates, a linear relationship between t versus Z was obtained (Fig. 13). The respective values of K and N_0 calculated from the slope and intercept of the linear plot are presented in Table 7. From the table, it is evident that the maximum sorption capacity (N_0) decreased
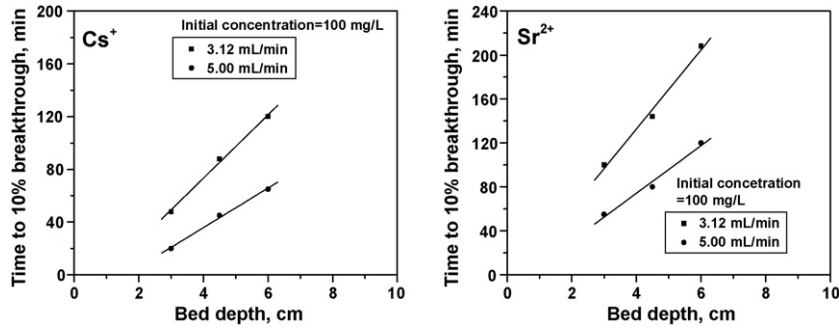
Fig. 13. BDST plots at 10% breakthrough for the removal of Cs$^+$ and Sr^{2+} ions at different flow rates on zeolite A.
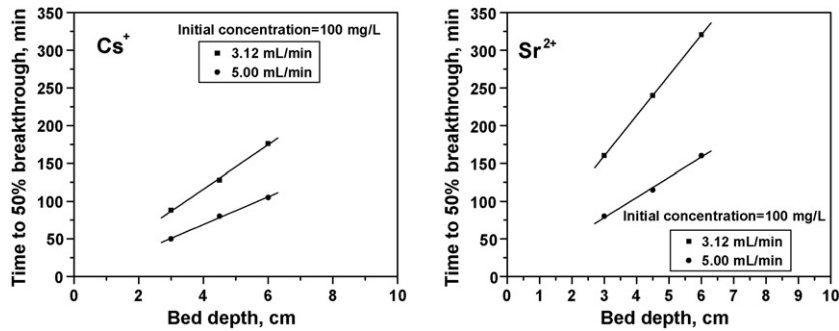

Fig. 14. BDST plots at 50% breakthrough for the removal of Cs$^+$ and Sr^{2+} ions at different flow rates on zeolite A.

with the increase in flow rate and the values of the sorption rate constant (K) were influenced by flow rate and increased with increase in flow rate indicating that external mass transfer dominated the overall system kinetics in the initial part of the sorption in the column. The critical bed depth (Z_0), which represent the theoretical depth of zeolite A material sufficient to prevent the Cs$^+$ and/or Sr^{2+} concentrations from exceeding C_b at $t = 0$, was estimated from Eq. (22). The obtained values of Z_0 (Table 7) were higher for the removal of Cs$^+$ ions than Sr^{2+} ions and these values increased with increase in flow rate.

At 50% breakthrough or $0.5(C/C_0)$, the logarithmic term in Eq. (19) reduces to zero, and the final term of BDST equation becomes zero, giving the relationship as in the following equation:

$$t_{1/2} = \frac{N_0}{C_0 U_0} Z \tag{23}$$

If the curve of $t_{1/2}$ (time to 50% breakthrough) versus Z is a straight line passing through the origin, it can be explained that the sorption data of both ions on the column follow the BDST model. Fig. 14 show that the data of the column studies follow BDST model as all the obtained straight lines nearly pass through the origin with a high correlation coefficient (R^2 above 0.99). Therefore, the bed performance such as the optimum bed depth and the service time of zeolite A in fixed bed column can be predicted from the equation of the BDST model. Consequently, the exchange capacity

Table 8
BDST model parameters of Cs$^+$ and Sr^{2+} ions sorbed onto zeolite A at different bed deaths and flow rates

Metal ion	Q (mL/min)	Z (cm)	Time to 50% breakthrough (min)	N_0 (mg/mL)	N_0 (mg/g)
Cs$^+$	3.12	3.0	88	11.64	16.40
		4.5	128		
		6.0	176		
	5.00	3.0	50	10.40	14.65
		4.5	80		
		6.0	105		
Sr^{2+}	3.12	3.0	160	21.24	29.91
		4.5	240		
		6.0	320		
	5.00	3.0	80	16.98	23.92
		4.5	115		
		6.0	160		

(N_0) at 50% breakthrough was calculated and presented in Table 8.

4. Conclusion

Synthetic zeolite A was tested as inorganic ion exchange material for the removal of cesium and strontium ions from aqueous chloride solutions. The kinetics of both metal ions was experimentally studied and the obtained rate data were analyzed using simple kinetic models. Results explained that the pseudo second-order sorption mechanism is predominant and the overall rate constant of each sorption process appears to be controlled by chemical sorption process. Equilibrium isotherms have been determined and tested for different isotherm expressions and the sorption data were successfully modeled using Langmuir, Freundlich, and Dubinin–Radushkviech (D–R) approaches. Based on the D–R model expression, the maximum sorption capacity and the mean free energy of the studied ions have been determined. The sorption of each ion is an endothermic process and spontaneous in nature. Fixed bed column sorption studies have shown that both studied ions removal was a strong function of initial flow rate, bed height and initial ion concentration. Increase in bed height and initial ion concentration resulted in decrease in effluent volume whereas increase in bed height leads to higher contact time thus higher effluent volume. Relatively higher sorption capacity and column performance were obtained for Sr^{2+} ions than Cs^+ ions. These reported results showed that synthetic zeolite A is an efficient ion exchange material for the removal of cesium and strontium ions from aqueous and wastewater solutions.

References

[1] E.S. Zakaria, I.M. Ali, I.M. El-Naggar, Thermodynamics and ion exchange equilibria of Gd $^{3+}$, Eu^{3+} and Ce^{3+} ions on H$^+$ form of titanium (IV) antimonate, Colloid Surf. A 210 (2002) 33–40.

[2] M.M. Abou- Mesalam, I.M. El-Naggar, Diffusion mechanism of Cs$^+$, Zn^{2+} and Eu^{3+} ions in the particles of zirconium titanate ion exchanger using radioactive tracers, Colloid Surf. A 215 (2003) 205–211.

[3] G. Atun, B. Bilgin, A. Kilislioglu, Kinetics of isotopic exchange between strontium polymolybdate and strontium ions in aqueous solution, Appl. Radiat. Isot. 56 (2002) 797–803.

[4] J. Lehto, R. Harjula, Selective separation of radionuclides from nuclear waste solutions with inorganic ion exchangers, Radiochim. Acta 86 (1999) 65–70.

[5] M.V. Sivaah, K.A. Venkatesan, R.M. Krishna, P. Sasidhar, G.S. Murthy, Ion exchange studies of europium on uranium antimonate, Colloid Surf. A 236 (2004) 147–157.

[6] T.J. Tranter, R.S. Herbst, T.A. Todd, A.L. Olson, H.B. Eldredge, Evaluation of ammonium molybdophosphate-polyacrylonitrile (AMP-PAN) as a cesium selective sorbent for the removal of ^{137}Cs from acidic nuclear waste solutions, Adv. Environ. Res. 6 (2002) 107–121.

[7] A. Nilchi, B. Maalek, A. Khanchi, M.G. Margheh, A. Bagheri, Cerium (IV) molybdate cation exchanger: synthesis, properties and ion separation capabilities, Radiat. Phys. Chem. 75 (2006) 301–308.

[8] A.M. El-Kamash, B. El-Gammal, A.A. El-Sayed, Preparation and evaluation of cerium (IV) tungstate powder as inorganic exchanger in sorption of cobalt and europium ions from aqueous solutions, J. Hazard Mater. 141 (2007) 219–228.

[9] R. Gwin, S.K. Das, S.K. Saha, Adsorption studies of zinc ions on barium titanate from aqueous solutions, Radiochem. Acta 90 (2002) 53–56.

[10] I.M. Ismail, M.R. El-Sourougy, N. Abdel Moneim, H.F. Aly, Equilibrium and kinetics studies of the sorption of cesium by potassium nickel hexacyanoferrate complex, J. Radioanl. Nucl. Chem. 240 (1999) 59–67.

[11] I.M. Ismail, M.R. El-Sourougy, N. Abdel Moneim, H.F. Aly, Preparation, characterizat- ion, and utilization of potassium nickel hexacyanoferrate for the separation of cesium and cobalt from contaminated waste water, J. Radioanl. Nucl. Chem. 237 (1998) 97–102.

[12] E.I. Shabana, M.I. El-Dessouky, Sorption of cesium and strontium ions on hydrous titanium dioxide from chloride medium, J. Radioanl. Nucl. Chem. 253 (2002) 281–284.

[13] K.M. Abd El-Rahman, A.M. El-Kamash, M.R. El-Sourougy, N.M. Abdel-Moniem, Thermodynamic modeling for the removal of Cs$^+$, Sr^{2+}, Ca^{2+}, and Mg^{2+} ions from aqueous waste solutions using zeolite A, J. Radioanl. Nucl. Chem. 268 (2006) 221–230.

[14] A.M. El-Kamash, A.A. Zaki, M. Abd El Geleel, Modeling batch kinetics and thermodynamics of zinc and cadmium ions removal from waste solutions using synthetic zeolite A, J. Hazard Mater. 127 (2005) 211–220.

[15] P.K. Sinha, K.B. Lal, P.K. Panicker, V. Krishnasamy, A comparative study on indigenously available synthetic zeolites for removal of strontium from solutions by ion-exchange, Radiochem. Acta 7 (1996) 157.

[16] A. Dyer, A.S. Abdel Gawad, M. Mikhail, H. Enamy, M. Afshang, The natural zeolite, laumontite, as a potential material for the treatment of aqueous nuclear wastes, J. Radioanal. Nucl. Chem. 4 (1991) 265–276.

[17] S.K. Durrani, A. Dyer, R. Blackburn, Self-diffusion of barium and cesium cations in neutron-and gamma-irradiated high-silica zeolites and boron–zeotypes, Zeolites 13 (1993) 1–13.

[18] K. Kotoh, T. Nishikawa, Y. Kashio, Multi-component adsorption characteristics of hydrogen isotopes on synthetic zeolite 5A-type at 77.4 K, J. Nucl. Sci. Technol. 39 (2002) 435–441.

[19] V.J. Inglezakis, M.D. Loizidon, H.P. Grigoropoulou, Equilibrium and kinetic ion exchange studies of Pb^{2+}, Cr^{3+}, Fe^{3+} and Cu^{2+} on natural clinoptilolite, Water Res. 36 (2002) 2784–2792.

[20] M.A.S.D. Barros, P.A. Arroyo, Thermodynamics of the exchange processes between K$^+$, Ca^{2+} and Cr^{3+} in zeolite NaA, Adsorption 10 (2004) 227–235.

[21] R. Qadeer, J. Hanif, I. Hanif, Uptake of thorium ions from aqueous solutions by zeolite molecular sieves (13X type) powder, J. Radioanal. Nucl. Chem. 190 (1995) 103–112.

[22] P.K. Sinha, K.B. Lal, P.K. Panieker, V. Krishnasamy, A comparative study on indigenously available synthetic zeolites for removal of strontium from solution by ion-exchange, Radiochem. Acta 73 (1996) 157–163.

[23] S. Ouki, M. Kavannagh, Performance of natural zeolites for the treatment of mixed metal-contaminated effluents, Waste Manage Res. 15 (1997) 383–391.

[24] E. Chmielewska, A. Horvathova, The interaction mechanisms between aqueous solutions of ^{137}Cs and ^{134}Ba radionuclides and local natural zeolites for reaction scenario, J. Radioanal. Nucl. Chem. 227 (1998) 151–155.

[25] S. Goni, A. Guerrero, M.P. Lorenzo, Efficiency of fly ash belite cement and zeolite matreices for immobilizing cesium, J. Hazard. Mater. B137 (2006) 1608–1617.

[26] S. Amini, A. Dayer, S.K. Durrani, Fixation of actinides into zeolites/zeotype and flexcrete-cement matrix, J. Radioanal. Nucl. Chem. 173 (1993) 331–337.

[27] M. Foldsova, P. Luckac, Leachability of Co and Cs from natural and chemically treated zeolites, J. Radioanal. Nucl. Chem. 214 (1996) 479–487.

[28] A. Dyer, T. Las, M. Zubair, The use of natural zeolites for radioactive waste treatment studies on leaching from zeolite/cement composites, J. Radioanal. Nucl. Chem. 243 (2001) 839–841.

[29] Junfeng Li, Z.W. Gong, W. Jianlong, Solidification of low level-radioactive resins in ASC zeolite blends, Nucl. Eng. Design 235 (2005) 817–821.

[30] A.M. El-Kamash, M.R. El-Naggar, M.I. El-Dessouky, Immobilization of cesium and strontium radionuclides in zeolite-cement blends, J. Hazard. Mater. 136 (2006) 310–316.

[31] A.E. Osmanlioglu, Treatment of radioactive liquid waste by sorption on natural zeolite in Turkey, J. Hazard. Mater. 136 (2006) 310–316.

[32] S. Bagosi, L.J. Csetenyi, Immobilization of cesium-loaded ion exchange resins in zeolite-cement blends, Cem. Conc. Res. 29 (1999) 479–485.

[33] G.P.C. Rao, S. Satyaveni, A. Ramesh, K. Seshaiah, K.S.N. murthy, N.V. Choudary, Sorption of cadium and zinc from aqueous solutions by zeolite 4A, zeolite 13X and bentonite, J. Environ. Manag. 81 (2006) 265–272.

[34] M. Trogo, j. Peri, Interaction of the zeolite tuff with Zn-containing simulated pollutant solutions, J. Colliod Interface Sci. 260 (2003) 166–175.

[35] Y.S. Ho, G. McKay, A kinetics study of dye sorption by biosorbent waste product pith, Resour. Conserv. Recycl. 25 (1999) 171–193.

[36] G. McKay, Y.S. Ho, The sorption of lead (II) on peat, Water Res. 33 (1999) 585–587.

[37] G. McKay, Y.S. Ho, Pseudo-second order model for sorption processes, Process Biochem. 34 (1999) 451–460.

[38] F. Helfferich, Ion Exchange, Mc Graw Hill, New York, 1962.

[39] G.E. Boyd, A.W. Adamson, L.S. Mayers, The exchange adsorption of ions from aqueous solutions by zeolites. II. Kinetics, J. Am. Chem. Soc. 69 (1947) 28–36.

[40] D. Rechenberg, Properties of ion-exchange resin in relation to their structure. III. Kinetics of exchange, J. Am. Chem. Soc. 75 (1953) 589–601.

[41] G.M. Walker, L.R. Weatherly, Kinetics of acid dye adsorption on GAC, Water Res. 33 (1999) 1895–1899.

[42] K.G. Scheckel, D.L. Sparks, Temperature effects on nickel sorption kinetics at mineral water interface, Soil. Sci. Soc. Am. J. 65 (2001) 719–728.

[43] J. Peric, M. trgo, N.V. Medvidovic, Removal of zinc, copper and lead by natural zeolite- a comparison of adsorption isotherms, Water Res. 38 (2004) 1839–1899.

[44] D. Mohan, S. Chander, Single, binary, and multi component sorption of iron and manganese on lignite, J. Colloid Interface Sci. 299 (2006) 57–76.

[45] D. Mohan, K.P. Singh, Single and multi-component adsorption of cadmium and zinc using activated carbon derived from bagasse an agricultural waste, Water Res. 36 (2002) 2304–2318.

[46] M.I. Panayotova, Kinetics and thermodynamics of copper ions removal from wastewater by use of zeolite, Waste Manag. 21 (2001) 671–676.

[47] S. Netpradit, P. Thiravetyan, S. Towprayoon, Evaluation of metal hydroxide sludge for reactive dye adsorption in a fixed-bed column system, Water Res. 38 (2004) 71–78.

[48] S. Kundu, A.K. Gupta, As(III) removal from aqueous medium in fixed bed using iron oxide-coated cement (IOCC): Experimental and modeling studies, Chem. Eng. J. (2006).

[49] T.S. Singh, K.K. Pant, Experimental and modeling studies on fixed bed adsorption of As(III) ions from aqueous solution, Sep. & Purif. Technol. 48 (2006) 288–296.

[50] U. Kumar, M. Bandyopadhyay, Fixed bed study for Cd(II) removal from wastewater using treated rice husk, J. Hazard. Mater. 129 (2006) 253–259.

[51] G.S. Bohart, E.Q. Adams, Some aspects of the behavior of charcoal with respect to chlorine, J. Am. Chem. Soc. 42 (1920) 523–544.

[52] E. Malkoc, Y. Nuhoglu, Removal of Ni(II) ions from aqueous solutions using waste of tea factory: adsorption on a fixed bed column, J. Hazard. Mater. 135 (2006) 328–336.